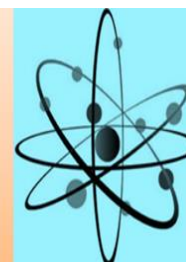




## Journal of Physical Chemistry and Functional Materials (JPCFM)

journal homepage: <http://dergipark.gov.tr/jphcfum>



Received: 30 July 2018

Accepted: 31 July 2018

Research Article

### Zinc Ferrite Films Doped with Lanthanides for Gas Sensor Application

Sevda Saritas<sup>a\*</sup>, Erdal Turgut<sup>b</sup>, Bekir Gurbulak<sup>c</sup>, Mutlu Kundakci<sup>c</sup>, Muhammet Yildirim<sup>c</sup>

<sup>a</sup>Department of Electrical and Energy, Ispir Hamza Polat Vocational School of Higher Education, Ataturk University, 25250, Erzurum, Turkey.

<sup>b</sup>Department of Electrical and Energy, Aşkale Vocational School of Higher Education, Ataturk University, 25250, Erzurum, Turkey.

<sup>c</sup>Department of Physics, Ataturk University, 25250, Erzurum, Turkey.

\*Corresponding Author: [sevda.saritas76@gmail.com](mailto:sevda.saritas76@gmail.com)

#### Abstract

In this study, it was tried to make the zinc ferrite ( $Zn_xFe_{3-x}O_4$ ) films with lanthanides such as dysprosium (Dy) and erbium (Er) doping a very cheap and easy method, Chemical Spray Pyrolysis Technique (CSP) to have suitable properties for application. The lanthanides are located in block 5d of the periodic table. Gas sensors can be made from various materials depending on the purposes they serve. Regardless type of gas sensor, general requirements for a reliable gas sensor is high sensitivity, fast response, and good selectivity. It was found that  $Zn_xFe_{3-x}O_4$  films with Dy and Er doping thin films operating at 200°C temperature could detect  $H_2$  at 100 ppm, 500 ppm and 1000 ppm concentration and at 1800 s time with very low selectivity and sensitivity relatively. X-Ray Diffraction (XRD) measurements of the obtained films were taken between 10 and 70 degrees. As a result of Atomic Force Microscope (AFM) measurements, was obtained information about surface morphology. Optical properties were measured by Double-Diffracted UV-VIS photoelectron spectroscopy. I-V (Van der Pauw) technique has been used for response of gas sensor.

**Key Words:** Zinc Ferrite, Chemical Spray Pyrolysis Technique (CSP), Lanthanide metals.

## Introduction

Interest in detecting and determining concentrations of toxic gases has constantly been on the increase in recent years due to increase of industrial enterprise. Metal oxide gas sensors are among most important devices to detect a large variety of gases.  $\alpha$ - $\text{Fe}_2\text{O}_3$ , an environmental friendly semiconductor ( $E_g = 2.1 \text{ eV}$ ), is the most stable iron oxide under ambient atmosphere [1].

Because of its low cost, high stability, high resistance to corrosion, and its environmentally friendly properties is one of the most important metal oxides for gas sensing applications. Various chemical pollutants have been released in high quantities into the atmosphere as a result of human activities and have generated environmental risks one of the critical factors that contribute to global warming and harm to human health.

In order to monitor air pollution on a large scale, inexpensive, reliable and easy to use gas sensors are needed. The electrical resistance of semiconductor oxides, such as  $\text{SnO}_2$ ,  $\text{ZnO}$ ,  $\text{TeO}_2$ ,  $\text{WO}_3$  and  $\text{Fe}_2\text{O}_3$ , has a strong dependence on the concentration of surrounding gases.

According to this principle, these oxides are commercially designed as chemical sensors to detect toxic gases such as LPG,  $\text{NO}_2$ ,  $\text{H}_2$ ,  $\text{O}_2$ ,  $\text{CO}$ ,  $\text{H}_2\text{O}$  [2,3].

## Materials and methods

### Synthetic procedures;

Chemical spray pyrolysis (CSP) is one of the solution based coating technique to produce metallic and semiconductor thin or thick films. The technique of CSP (Fig. 1) without the requirement of vacuum is a method that can be preferred in the industry, in order to allow the production of large size films in both cheap. Many parameters such as substrate temperature, the salts (Table 1), molarity and deposition time have carefully been chosen to obtain the best growth condition in this technique. The substrate was sprayed with argon gas onto a substrate heated to  $320 \text{ }^\circ\text{C}$  at a distance of 30 cm. All films grown times were 35 min.

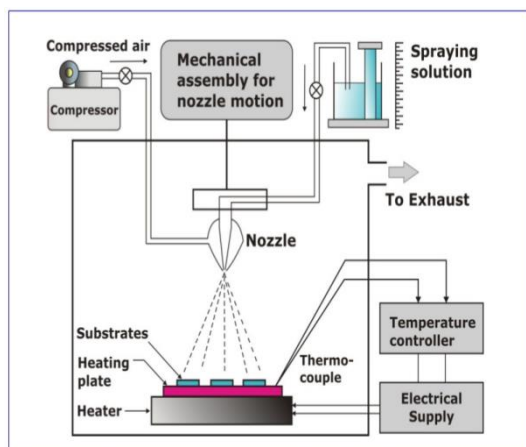


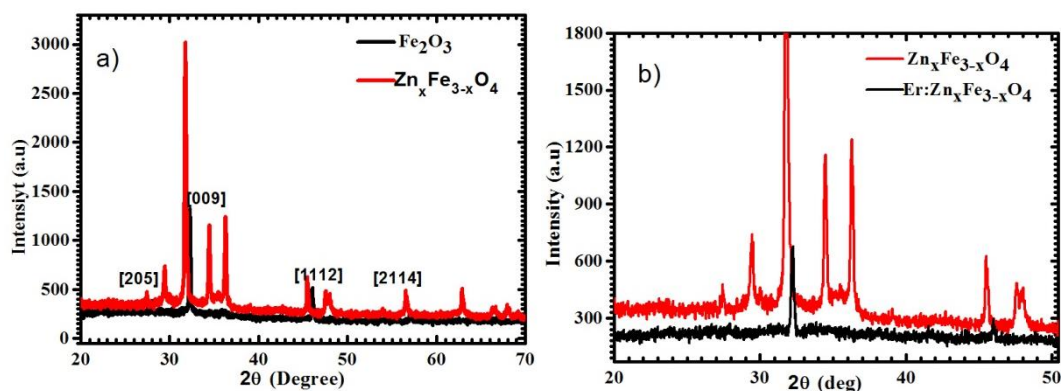
Fig. 1. Schematic diagram of Chemical spray pyrolysis system

Table 1. Table of salt for the preparation of nanostructured

Film	Used Chemical Salt	Solution Ratio	Molar Ratio
$Zn_xFe_{3-x}O_4$	$FeCl_3 \cdot 6H_2O + FeCl_2 \cdot 4H_2O + NaOH + Zn(NO_3)_2 \cdot 6H_2O$	1:2:0.25:0.1	
$Fe_2O_3$	$FeCl_3 \cdot 6H_2O + FeCl_2 \cdot 4H_2O + NaOH +$	1:2:0.25	
Er: $Zn_xFe_{3-x}O_4$	$FeCl_3 \cdot 6H_2O + FeCl_2 \cdot 4H_2O + NaOH + Zn(NO_3)_2 \cdot 6H_2O + Er(NO_3)_3 \cdot 6H_2O$	1:2:0.25:0.1:0.01	
Dy: $Zn_xFe_{3-x}O_4$	$FeCl_3 \cdot 6H_2O + FeCl_2 \cdot 4H_2O + NaOH + Zn(NO_3)_2 \cdot 6H_2O + Dy(NO_3)_3 \cdot 6H_2O$	1:2:0.25:0.1:0.01	

## Result and discussion

The morphologic and structure (particle size, pore size, etc.) properties of  $Zn_xFe_{3-x}O_4$ ,  $Fe_2O_3$ , Er: $Zn_xFe_{3-x}O_4$  and Dy: $Zn_xFe_{3-x}O_4$  thin films have been generally and carefully investigated. XRD and AFM (for topographic properties) techniques have been used for structural analysis and I-V (Van der Pauw) technique has been used for response of gas sensor. According to XRD (Fig. 2) measurements, the crystal structure of the materials have changed.



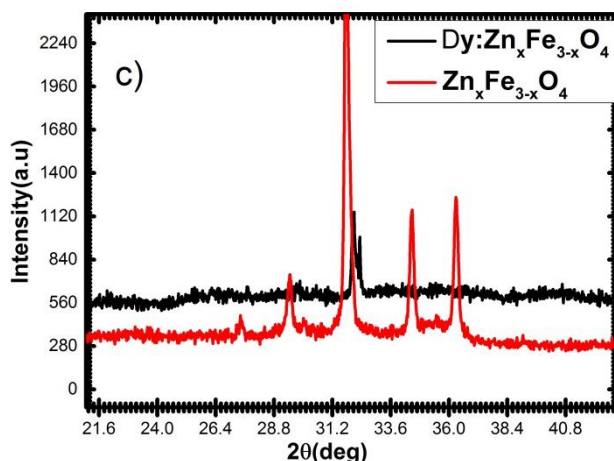


**Fig. 2.** XRD patterns of a)  $\text{Fe}_2\text{O}_3$ ,  $\text{Zn}_x\text{Fe}_{3-x}\text{O}_4$ , b)  $\text{Er}:\text{Zn}_x\text{Fe}_{3-x}\text{O}_4$  and c)  $\text{Dy}:\text{Zn}_x\text{Fe}_{3-x}\text{O}_4$  thin films (Reference code 01-073-1963, 00-015-0615).

In Fig.3, a)  $\text{Fe}_2\text{O}_3$  and  $\text{Zn}_x\text{Fe}_{3-x}\text{O}_4$  b)  $\text{Er}:\text{Zn}_x\text{Fe}_{3-x}\text{O}_4$  and c)  $\text{Dy}:\text{Zn}_x\text{Fe}_{3-x}\text{O}_4$  thin films band gap are calculated 2.16 eV, 2.14 eV, 2.04 eV, 2.16 eV respectively. As Mg doped Iron Oxide thin films gives absorption at smaller wave lengths, it shifts at larger wave length as a result of doping. It can be said that the energy band gap is causing the band gap to narrow due to the fact that the imperfections in the structure may pass at the band edge.

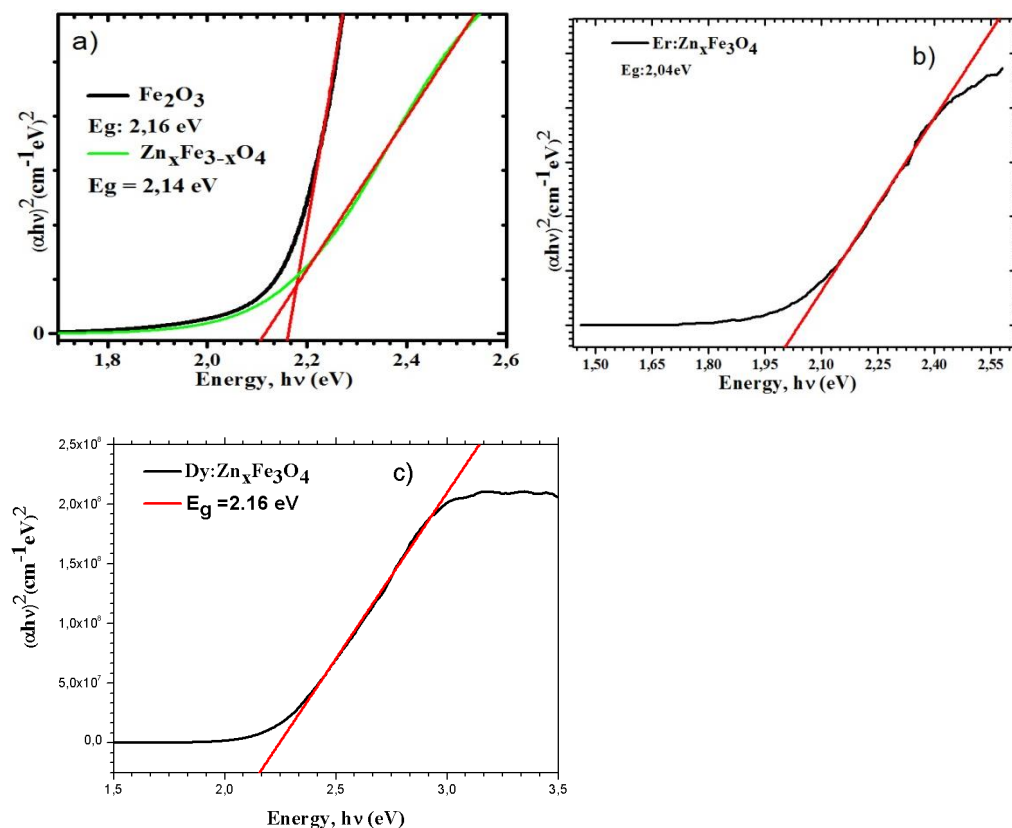


**Fig.3.** Plot of  $(\alpha h\nu)^2(\text{cm}^{-1}\text{eV})^2$  versus photon energy  $h\nu$  of a)  $\text{Fe}_2\text{O}_3$ ,  $\text{Zn}_x\text{Fe}_{3-x}\text{O}_4$  b)  $\text{Er}:\text{Zn}_x\text{Fe}_{3-x}\text{O}_4$  and c)  $\text{Dy}:\text{Zn}_x\text{Fe}_{3-x}\text{O}_4$  thin films

AFM images of the Fig 4a)  $\text{Fe}_2\text{O}_3$ , 4b)  $\text{Zn}_x\text{Fe}_{3-x}\text{O}_4$ , 4c) Er:  $\text{Zn}_x\text{Fe}_{3-x}\text{O}_4$  and 4d) Dy:  $\text{Zn}_x\text{Fe}_{3-x}\text{O}_4$  thin films grown on glass substrates have been observed that line roughness value of film is change with doping Dy, Er and Zn metals. And so, gas response of the films change with crystal size. The  $\text{Fe}_2\text{O}_3$  films line roughness value is about 28,6 nm. The  $\text{Zn}_x\text{Fe}_{3-x}\text{O}_4$  films line roughness value is about 34 nm.

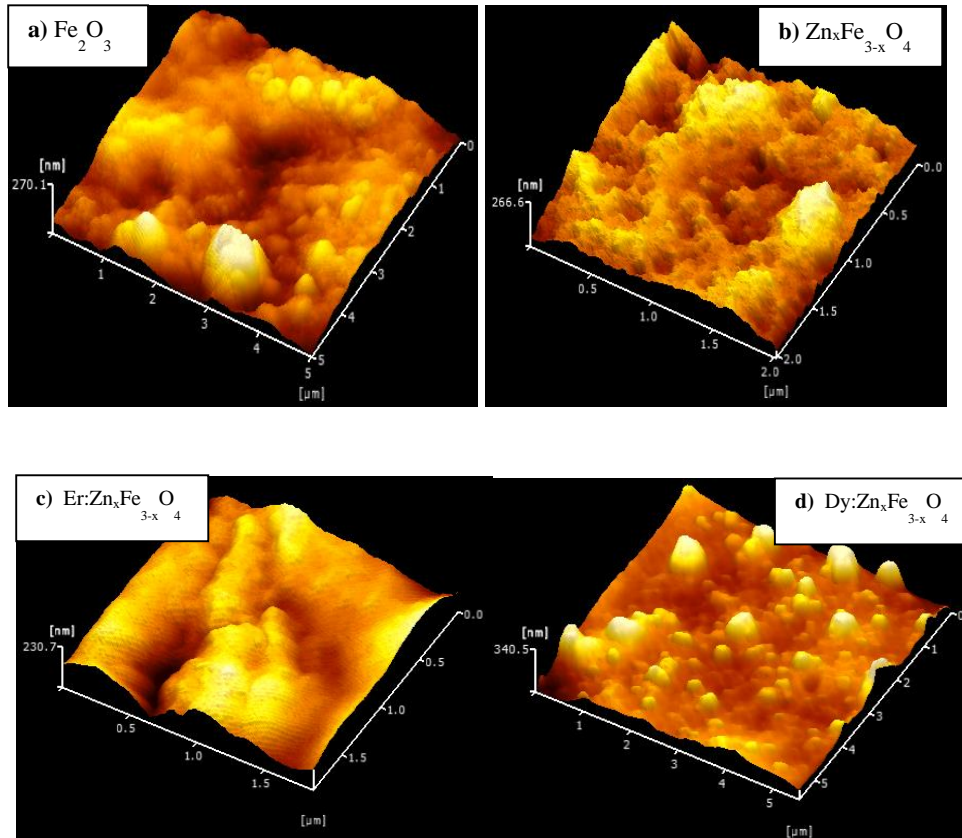


**Fig.4.** Three dimensional AFM images of a)  $\text{Fe}_2\text{O}_3$ , b)  $\text{Zn}_x\text{Fe}_{3-x}\text{O}_4$ , c)Er:  $\text{Zn}_x\text{Fe}_{3-x}\text{O}_4$  and d) Dy:  $\text{Zn}_x\text{Fe}_{3-x}\text{O}_4$  thin films

The Dy:  $\text{Zn}_x\text{Fe}_{3-x}\text{O}_4$  films line roughness value is about 17.4 nm. The Er:  $\text{Zn}_x\text{Fe}_{3-x}\text{O}_4$  films line roughness value is about 24.6 nm

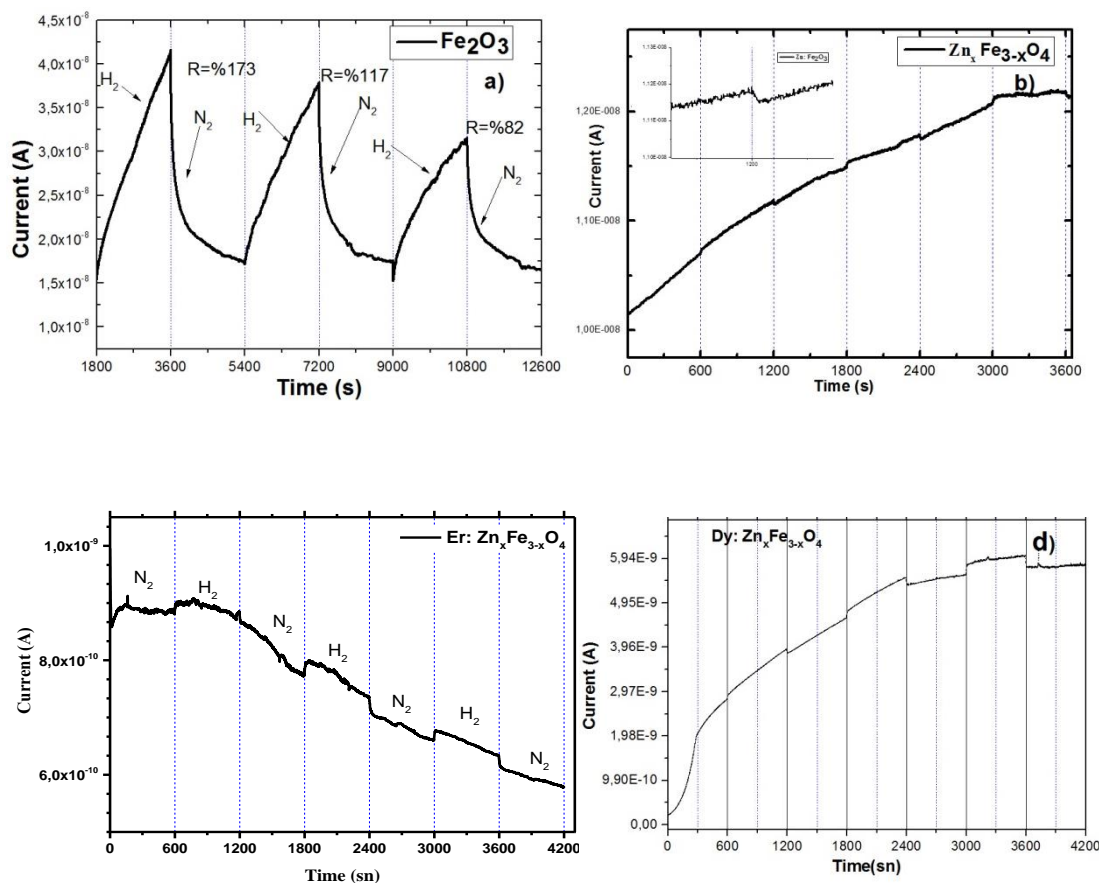


**Fig. 5. Sensor Response of a)  $\text{Fe}_2\text{O}_3$ , b)  $\text{Zn}_x\text{Fe}_{3-x}\text{O}_4$ , c)  $\text{Er: Zn}_x\text{Fe}_{3-x}\text{O}_4$  and d)  $\text{Dy: Zn}_x\text{Fe}_{3-x}\text{O}_4$  thin films**

**Table 2. Respons of the gas sensors**

Time	1800.s (100 ppm)	1800.s (500 ppm)	1800.s (1000 ppm)
$\text{Fe}_2\text{O}_3$	%R= 173	%R= 117	%R= 82
Time	600.s (100 ppm)	600.s (500 ppm)	600.s (1000 ppm)
$\text{Zn}_x\text{Fe}_{3-x}\text{O}_4$	%R= 0.10	%R =0.17	%R= 0.20

$\%R = (I_0 - I) / I_0 \cdot 100$ ;  $R$  sensors respons,  $I_0$ ; first current,  $I$ ; finally current. According to calculations made, Table 2 gives the respons of the gas sensors

$\text{Fe}_2\text{O}_3$  show the time-dependent change in the gas response of the thin film to hydrogen gas, and the measurement is periodically 1800 s nitrogen and 1800 s hydrogen gas at  $200^\circ\text{C}$  (Fig.5). This measurement was made to evaluate the response of the thin film to hydrogen gas, and the  $\text{O}(\text{ads}) + 2\text{H}$

→  $\text{H}_2\text{O} + \text{e}^-$  [4] reaction of the film to hydrogen gas was found to be very high. During the measurement periodically 1800 s nitrogen and 1800 s hydrogen gas were supplied to the system at  $200^\circ\text{C}$  temperature. The film, which did not react to hydrogen gas at room temperature, reacted at a temperature of  $200^\circ\text{C}$ . Nitrogen was used as the sweeping gas. In the first 1800 s 500 ppm nitrogen swept system, 100 ppm hydrogen gas, second cycle 500 ppm for 1800 s hydrogen gas then nitrogen is swept in again and third cycle 1000 ppm for 1800 s hydrogen gas were supplied and the amount of current drawn by the system increased. This material is a promising material for gas sensor application. The same gauge is repeated for all films for 600 s, indicating that hydrogen is held at a lower level, which means that the hydrogen is stored in the structure, during which the hydrogen is separated from the structure in very small amounts.  $\text{Fe}_2\text{O}_3$  material is a promising material for gas sensor application as well as promising hydrogen storage applications [5-7].

### Conclusion

When we get the gas sensor response measure we detect that  $\text{Fe}_2\text{O}_3$ , Er:  $\text{Zn}_x\text{Fe}_{3-x}\text{O}_4$  and Dy:  $\text{Zn}_x\text{Fe}_{3-x}\text{O}_4$  thin films are the n type semiconductors and  $\text{Zn}_x\text{Fe}_{3-x}\text{O}_4$  is p type semiconductor and response time smaller and so faster than others. For  $\text{Fe}_2\text{O}_3$ , Er:  $\text{Zn}_x\text{Fe}_{3-x}\text{O}_4$  and Dy:  $\text{Zn}_x\text{Fe}_{3-x}\text{O}_4$  thin films, because of the electrons that emerge as a result of the reaction increase or decrease the carrier concentration.

### Acknowledgements

This work "Zinc Ferrite Films Doped With Lanthanides For Gas Sensor Application" has not been published in any scientific journals before. In this work, the properties of  $\text{Fe}_2\text{O}_3$ ,  $\text{Zn}_x\text{Fe}_{3-x}\text{O}_4$ , Er:  $\text{Zn}_x\text{Fe}_{3-x}\text{O}_4$  and Dy:  $\text{Zn}_x\text{Fe}_{3-x}\text{O}_4$  thin films were investigated. We can use this film for gas sensor application. I declare that there is no conflict of interest regarding the publication of this paper.

### References

- [1] M. Mishra, DM. Chun (2015)  $\alpha\text{-Fe}_2\text{O}_3$  as a photocatalytic material: A review. Applied Catalysis A: General 498: 126-141.
- [2] L.H. Huo, Q. Li, H. Zhao, L.J. Yu, S. Gao, J.G. Zhao Sol-gel route to pseudocubic shaped  $\alpha\text{-Fe}_2\text{O}_3$  alcohol sensor: preparation and characterization Sens. Actuators, B, 107 (2005), pp. 915-920
- [3] O.K. Tan, W. Cao, W. Zhu, J.W. Chai, J.S. Pan Ethanol sensors based on nano-sized  $\alpha\text{-Fe}_2\text{O}_3$  with  $\text{SnO}_2$ ,  $\text{ZrO}_2$ ,  $\text{TiO}_2$  solid solutions Sens. Actuators, B, 93 (2003), pp. 396-401
- [4] S. Saritas, M. Kundakci, Coban, O., Tuzemen, S., & Yildirim, M. (2018). Ni:  $\text{Fe}_2\text{O}_3$ , Mg:  $\text{Fe}_2\text{O}_3$  and  $\text{Fe}_2\text{O}_3$  thin films gas sensor application. *Physica B: Condensed Matter*, 541, 14-18.
- [5] M. Barroso, CA. Mesa, SR. Pendlebury, AJ. Cowan, Hisatomi T, (2012) Dynamics of photogenerated holes in surface modified  $\alpha\text{-Fe}_2\text{O}_3$  photoanodes for solar water splitting. PNAS 109: 15640-15645.

[6] M. Ni, MKH. Leung, DYC. Leung, K. Sumathy (2007) A review and recent developments in photocatalytic water-splitting using TiO<sub>2</sub> for hydrogen production. *Renew Sustain Energy Rev* 11: 401-425.

[7] K. Maeda, K. Domen (2007) New Non-Oxide Photocatalysts Designed for Overall Water Splitting under Visible Light. *J Phys Chem C* 111: 7851-7861.